The Full-Spectrum Correlated-*k* Distribution for Thermal Radiation From Molecular Gas-Particulate Mixtures

Michael F. Modest
Fellow ASME
e-mail: mfm6@psu.edu

Hongmei Zhang
Mem. ASME

Dept. of Mechanical Engineering,
Penn State University,
University Park, PA 96802

A new Full-Spectrum Correlated-k Distribution has been developed, which provides an efficient means for accurate radiative transfer calculations in absorbing/emitting molecular gases. The Full-Spectrum Correlated-k Distribution can be used together with any desired solution method to solve the radiative transfer equation for a small number of spectral absorption coefficients, followed by numerical quadrature. It is shown that the Weighted-Sum-of-Gray-Gases model is effectively only a crude implementation of the Full-Spectrum Correlated-k Distribution approach. Within the limits of the Full-Spectrum Correlated-k Distribution model (i.e., an absorption coefficient obeying the so-called "scaling approximation"), the method is exact. This is demonstrated by comparison with line-by-line calculations for a one-dimensional CO_2-N_2 gas mixture as well as a two-dimensional CO_2-H_2O-N_2 gas mixture with varying temperature and mole fraction fields.
[DOI: 10.1115/1.1418697]

Keywords: Combustion, Gaseous, Radiation

Introduction

Radiative heat transfer in gases has important applications from combustion systems to modeling atmospheric processes. The magnitude of radiative heat fluxes can have profound effects on combustion performance and environmental impact. Radiative heat transfer calculations in combustion gases may be loosely grouped into the following three methods (in order of decreasing complexity): (1) line-by-line calculations; (2) band models; and (3) global models.

Line-by-line calculations are the most accurate to date, but they require vast amounts of computer resources. This is undesirable even with the availability of powerful supercomputers, since radiative calculations are only a small part of a sophisticated fire/combustion code. Many studies have been devoted to narrow and wide band models, such as the Malkmus narrow band model, the correlated-*k* (CK) model and many others. The CK method is based on the fact that inside a spectral band $\Delta\eta$, which is sufficiently narrow to assume a constant Planck function, the precise knowledge of each line position is not required for the computation [1–7]. In this paper the CK approach is extended to the whole spectrum by defining a Planck function weighted cumulative *k*-distribution function.

The most common global method is the so-called Weighted-Sum-of-Gray-Gases model. The concept of the WSGG approach was first presented by Hottel and Sarofim [8] within the framework of the zonal method. The method could be applied to arbitrary geometries with varying absorption coefficients, but was limited to nonscattering media confined within a black-walled enclosure. Modest [9] has shown that this model may be generalized for use with any arbitrary solution method. In this method the nongray gas is replaced by a number of gray gases, for which the heat transfer rates are calculated independently by solving the RTE with weighted emissive powers for each of the gray gases. The total heat flux is then found by adding the fluxes of all gray gases. The different absorption coefficient κ_i and emissive power weight factor for each gas are found from total emissivity data.

Denison and Webb [10–15] have improved on the WSGG model and have developed the Spectral-Line-Based Weighted-Sum-of-Gray-Gases (SLW) model based on detailed spectral line data. They also extended the SLW model to nonisothermal and nonhomogeneous media by introducing a cumulative distribution function of the absorption coefficient, calculated over the whole spectrum and weighted by the Planck function. The absorption distribution function (ADF) approach [16–18] is almost identical to the SLW model and differs from the SLW only in the calculation of the gray-gas weights. These weights are chosen in such a manner that emission by an isothermal gas is rigorously predicted for actual spectra. This method has been further generalized [17] by introducing fictitious gases (ADFFG) employing a joint distribution function that separates the κ_η into two or more fictitious gases, and is designed to be more suitable for the treatment of nonhomogeneous media.

In this paper, the Full-Spectrum Correlated-*k* Distribution approach is developed based on Weighted-Sum-of-Gray-Gases arguments. This approach provides a smoother—and, therefore, more easily integrated—set of weight functions than the ADF method. Through these arguments the Weighted-Sum-of-Gray-Gases model is shown to be simply a crude implementation of the FSCK (Full-Spectrum Correlated-*k* Distribution) developed here. Therefore, it is clear that the WSGG method, like the correlated-*k* approach, is not limited to black-walled enclosures without scattering [9], but can accommodate gray walls as well as gray scattering particles. This is also shown through direct WSGG arguments.

Theoretical Formulation

Consider an absorbing/emitting medium inside a black enclosure. For simplicity, we will first assume here that the medium does not scatter, and that it consists primarily of molecular combustion gases (such as H_2O and CO_2 mixed in air) with their thousands of spectral lines, plus perhaps some non-scattering particles, such as soot, all enclosed by opaque black walls. However,

Contributed by the Heat Transfer Division for publication in the JOURNAL OF HEAT TRANSFER. Manuscript received by the Heat Transfer Division November 28, 2001; revision received June 1, 2001. Associate Editor: J. P. Gore.

this approach is also valid for gray scattering and/or gray walls, which will be shown later. For such a situation the radiative equation of transfer (RTE) is given by [19]

$$\frac{dI_\eta}{ds}=\kappa_\eta(I_{b\eta}-I_\eta), \tag{1}$$

where I_η is the spectral intensity varying along a path s, η is wavenumber, $I_{b\eta}$ the Planck function, and κ_η is the spectral absorption coefficient, which (besides wavenumber) depends on local temperature T, pressure p and mole fractions $\underline{x}$. This is the starting point to make line-by-line calculations. The formal solution to Eq. (1) is [19]

$$I_\eta(s)=I_{bw\eta}e^{-\int_0^s\kappa_\eta ds''}+\int_0^s I_{b\eta}(T(s'))e^{-\int_{s'}^s\kappa_\eta ds''}\kappa_\eta(s')ds', \tag{2}$$

where the subscript w denotes a value at the wall. Integrated over the entire spectrum this becomes [9]

$$\begin{aligned}I(s)&=\int_0^\infty I_\eta d\eta\\&=I_{bw}[1-\alpha(T_w,0\to s)]\\&\quad+\int_0^s I_b(s')\frac{\partial\alpha}{\partial s'}(T(s'),s'\to s)ds',\end{aligned} \tag{3}$$

where

$$\alpha(T,s'\to s)=\frac{1}{I_b(T)}\int_0^\infty I_{b\eta}(T)[1-e^{-\int_{s'}^s\kappa_\eta ds''}]d\eta \tag{4}$$

is the total absorptivity for a gas column $s'\to s$ for irradiation from a blackbody source at temperature T. We will now assume that the commonly used ''scaling approximation'' applies, i.e., that spectral and spatial dependence of the absorption coefficient are separable,

$$\kappa_\eta(\eta,T,p,\underline{x})=k_\eta(\eta)u(T,p,\underline{x}). \tag{5}$$

This approximation is used, for example, in the popular Curtis-Godson approximation to calculate narrow band absorptivities for nonhomogeneous paths [20], and in correlated-k models applied to nonhomogeneous atmospheres [3,21]. While a good approximation for soot, its accuracy is more limited for molecular gases: if we assume spectral lines of Lorentz shape we get [19]

$$\kappa_\eta(\eta,T,p,\underline{x})=\sum_j\frac{S_j}{\pi}\frac{b_j}{(\eta-\eta_j)^2+b_j^2}, \tag{6}$$

where η_j is the spectral position of the center of the j^{th} line, b_j is the line's half width at half height, and S_j is the line's intensity. In order for Eq. (5) to hold, we need all b_j to be constant (usually fairly true if total pressure is constant) and all S_j to have the same spatial dependence (the S_j depend only on temperature and density of the absorbing species). Equation (5) has been shown to give very accurate results in atmospheric applications, even for strong variations in total pressure [2,21], but—due to hot lines with strongly different temperature dependence of the line intensities—may become less accurate in the presence of fields with extreme temperature variations [4,6,22]. Moreover, the line intensities are directly proportional to the partial pressure of the absorbing gas. Thus, in gas mixtures with locally varying mole fraction ratios, Eq. (5) is also certain to be violated.

Sticking Eq. (5) into Eqs. (2) and (4) yields

$$I_\eta(s)=I_{bw\eta}e^{-k_\eta X(0,s)}+\int_0^s I_{b\eta}(s')e^{-k_\eta X(s',s)}k_\eta u(s')ds', \tag{7}$$

$$\alpha(T,s'\to s)=\frac{1}{I_b(T)}\int_0^\infty I_{b\eta}[1-e^{k_\eta X(s',s)}]d\eta, \tag{8}$$

where

$$X(s',s)=\int_{s'}^s u(s'')ds''. \tag{9}$$

In the k-distribution method it is recognized that—over a small spectral interval over which $I_{b\eta}$ may be assumed constant—the absorption coefficient attains the same value many times. If the medium is homogeneous [i.e., $\kappa_\eta=\kappa_\eta(\eta)$ only], and even in a nonhomogeneous medium if Eq. (5) applies, the absorption coefficient may be reordered into a monotonically increasing function without loss of accuracy. For a narrow spectral interval we then write for the narrow band transmissivity $\overline{\tau}_\eta$

$$\overline{\tau}_\eta=\frac{1}{\Delta\eta}\int_{\Delta\eta}e^{-k_\eta X}d\eta=\int_0^\infty e^{-kX}f(k)dk=\int_0^1 e^{-k(g)X}dg, \tag{10}$$

where the cumulative k-distribution

$$g(k)=\int_0^k f(k)dk \tag{11}$$

is an equivalent, nondimensional wavenumber. In Eq. (10) the integration can be switched from η to k_η, since for each η there is only a single value of k_η (but many different η for each k_η).

A similar argument can be applied to the entire spectrum. Defining a fractional Planck function as

$$i(T,\eta)=\frac{1}{I_b(T)}\int_0^\eta I_{b\eta}d\eta, \tag{12}$$

it is obvious that $i(T,0)=0$ and $i(T,\infty)=1$, i.e., the fractional Planck function is monotonically increasing with $0\leqslant i\leqslant 1$. Equation (8) can then be rewritten as

$$\alpha(T,s'\to s)=1-\tau(T,s'\to s)=1-\int_0^1 e^{-k_\eta(i)X(s',s)}di. \tag{13}$$

We note there is only one value of k_η for each value of i (but many values of i for a single value of k_η). Thus, we may reorder Eq. (13) in the same way as Eq. (10), leading to

$$\tau=\int_0^1 e^{-k_\eta(i)X}di=\int_0^\infty e^{-kX}f(T,k)dk=\int_0^1 e^{-k(T,g)X}dg. \tag{14}$$

Here, g is no longer an equivalent wavenumber, but an equivalent fractional Planck function. Note that, since i is a function of temperature, so is k, i.e. $k=k(T,g)$. Since we would like to be able to use arbitrary methods for the solution of the radiative transfer problem, employing the simplified $k-g$ relation of Eq. (14) (rather than $k_\eta-\eta$), the temperature dependence of $k(T,g)$ is rather inconvenient. Following Modest [9] we desire a form, which, upon substitution into Eq. (3), can be shown to reduce back to the original RTE, Eq. (1). We will, therefore, carry out one more reordering step to modify Eq. (14) to

$$\tau=\int_0^1 e^{-k(T,g)X}dg=\int_0^1 a(T,g_{\text{ref}})e^{-k(T_{\text{ref}},g_{\text{ref}})X}dg_{\text{ref}}, \tag{15}$$

where $k(T_{\text{ref}},g_{\text{ref}})$ is the $k-g$ distribution evaluated at a reference temperature T_{ref}, i.e., we have moved the temperature dependence from the exponent (in k) to a base function a. How this is done is best understood by looking at Fig. 1, which shows two typical k-distributions for T_{ref} (the reference temperature) and some other temperature T. Both functions have identical values for $k=k_{\min}$ at $g=0$ (the minimum absorption coefficient across the spectrum, usually zero), and $k=k_{\max}$ at $g=1$ (the maximum absorption co-

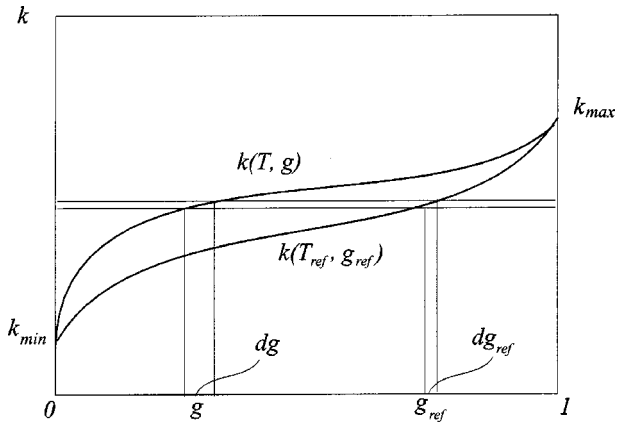

Fig. 1 The weight function *a*, obtained from *k*-distributions at different temperatures

efficient across the spectrum); for each value of k the corresponding value for g is simply shifted. Now setting $k(T,g) = k(T_{\mathrm{ref}},g_{\mathrm{ref}})$, and differentiating leads to

$$dg = \frac{\partial k(T_{\mathrm{ref}},g_{\mathrm{ref}})/\partial g_{\mathrm{ref}}}{\partial k(T,g)/\partial g} dg_{\mathrm{ref}} = \frac{f[T,k(g)]}{f[T_{\mathrm{ref}},k(g_{\mathrm{ref}})]} dg_{\mathrm{ref}} = a(T,g_{\mathrm{ref}})dg_{\mathrm{ref}}, \tag{16}$$

where we have arbitrarily set $a(T_{\mathrm{ref}},g_{\mathrm{ref}}) \equiv 1$ at the reference condition.

For simplicity of notation we will, from now on, drop the subscript "ref" from g_{ref}, as well as the argument T_{ref} from $k(T_{\mathrm{ref}},g_{\mathrm{ref}})$, which then is simply written as $k(g)$. Substituting Eq. (15) into Eq. (3), and noting that

$$\frac{\partial \alpha}{\partial s'} = -\frac{\partial \tau}{\partial s'} = \int_0^1 a(T,g) e^{-k(g)X(s',s)} k(g) \frac{\partial X}{\partial s'} dg = -\int_0^1 a(T,g) e^{-k(g)X} k(g) u(s') dg,$$

we obtain

$$I(s) = I_{bw} \int_0^1 a(T_w,g) e^{-kX(0,s)} dg + \int_0^s I_b(s') \int_0^1 a[T(s'),g] e^{-k(g)X(s',s)} k(g) u(s') dg ds'. \tag{17}$$

If we now introduce a new "spectral" intensity $I_g(s)$, we get

$$I(s) = \int_0^1 I_g(s) dg = \int_0^1 \left\{ [a(T_w,g) I_{bw}] e^{-kX(0,s)} + \int_0^s [a(T(s'),g) I_b(s')] \times e^{-kX(s',s)} k u(s') ds' \right\} dg. \tag{18}$$

Comparing with Eq. (7) we find that I_g satisfies the general RTE, Eq. (1), subject to the same boundary conditions, but for a spectrally-integrated, gray case with the Planck function replaced by a weighted value, $[aI_b]$:

$$\frac{dI_g}{ds} = k(g) u(s) ([aI_b] - I_g), \quad 0 \leqslant g \leqslant 1. \tag{19}$$

What remains to be done is to solve the gray medium RTE, Eq. (19), by any arbitrary solution method for a small number of gray absorption coefficients $k(g)$ (since k is a smooth, monotonic function in g), followed by numerical quadrature over I_g. In the correlated-k approach this is generally done by Gaussian quadrature, since this gives a high degree of accuracy with relatively few RTE evaluations. The most primitive (and least accurate) quadrature scheme would be the use of the trapezoidal rule; i.e.,

$$\int_0^1 I_g dg \simeq \sum_{i=1}^n I_g(k(g_i)) \Delta g_i; \quad \sum_{i=1}^n \Delta g_i = 1, \tag{20}$$

which would imply

$$\alpha = 1 - \tau = \int_0^1 a(T,g)(1 - e^{-k(g)X}) dg \simeq \sum_{i=1}^n A_i(T)(1 - e^{-k_i X}), \quad A_i = \int_{\Delta g_i} a dg, \tag{21}$$

which is commonly known as the "Weighted-Sum-of-Gray-Gases" (WSGG) method. Therefore, the Weighted-Sum-of-Gray-Gases method, while a very powerful method in itself, is effectively only a crude implementation of the Full-Spectrum Correlated-k approach presented here. Nevertheless, the WSGG method as presented in Eq. (21) was a considerable improvement over the previous state-of-the-art, which allowed only cumbersome and inaccurate application to inhomogeneous media [9,13,14].

Alternative Development. Equation (19) can also be derived directly from the spectral RTE, also including gray scattering and gray boundaries. Under the scaling approximation, the spectral RTE is then given by [19]

$$\frac{dI_\eta}{ds} = k_\eta u I_{b\eta} - (k_\eta u + \sigma_s) I_\eta + \frac{\sigma_s}{4\pi} \int_{4\pi} I_\eta(\hat{s}') \Phi(\hat{s},\hat{s}') d\Omega', \tag{22}$$

where σ_s is the scattering coefficient and $\Phi(\hat{s},\hat{s}')$ is the scattering phase function. In its most general form, Eq. (22) is subject to the boundary condition [19]

$$\text{at a wall,} \quad I_\eta = I_{w\eta} = \epsilon_w I_{bw\eta} + (1 - \epsilon_w) \frac{1}{\pi} \int_{\hat{\mathbf{n}}\cdot\hat{\mathbf{s}} \leq 0} I_\eta |\hat{\mathbf{n}} \cdot \hat{\mathbf{s}}| d\Omega, \tag{23}$$

where $I_{w\eta}$ is the spectral intensity leaving the enclosure wall, due to (diffuse gray) emission and/or (diffuse gray) reflection, ϵ_w is the emissivity of the wall, and $\hat{\mathbf{s}}$ and $\hat{\mathbf{n}}$ are unit vectors for direction and the surface normal (pointing out of the wall), respectively.

A redistributed RTE is obtained by multiplying Eq. (22) by $\delta(k - k_\eta)/f(T_{\mathrm{ref}},k)$, where $\delta(k - k_\eta)$ is the *Dirac-delta* function and

$$f(T_{\mathrm{ref}},k) = \frac{1}{I_b} \int_0^\infty I_{b\eta}(T_{\mathrm{ref}}) \delta(k - k_\eta) d\eta = \int_0^1 \delta(k - k_\eta) di \tag{24}$$

is the Planck-function-weighted k-distribution at the reference temperature, as already given in Eq. (14). Note that integrating the *Dirac-delta* function across a single occurrence of $k = k_\eta$ yields

$$\int \delta(k - k_\eta) d\eta = \int \delta(k - k_\eta) \frac{d\eta}{dk_\eta} dk_\eta = \left| \frac{d\eta}{dk_\eta} \right|. \tag{25}$$

Integrating the so-multiplied Eq. (22) across the spectrum, and assuming gray scattering properties yields the desired form

$$\frac{dI_g}{ds} = kuaI_b - (ku+\sigma_s)I_g + \frac{\sigma_s}{4\pi}\int_{4\pi} I_g(\hat{s}')\Phi(\hat{s},\hat{s}')d\Omega', \tag{26}$$

where

$$I_g = \int_0^\infty I_\eta \delta(k-k_\eta)d\eta \Big/ f(T_{\text{ref}},k), \tag{27a}$$

$$a = \frac{1}{I_b}\int_0^\infty I_{b\eta}\delta(k-k_\eta)d\eta \Big/ f(T_{\text{ref}},k) = f(T,k)/f(T_{\text{ref}},k), \tag{27b}$$

subject to the boundary condition

$$\text{at a wall,} \quad I_g = I_{wg} = \epsilon_w[a_g I_b](T_w) + (1-\epsilon_w)\frac{1}{\pi}\int_{\hat{\mathbf{n}}\cdot\hat{\mathbf{s}}<0} I_g|\hat{\mathbf{n}}\cdot\hat{\mathbf{s}}|d\Omega. \tag{28}$$

This reordering process requires that any factors accompanying radiative intensity I_η—with the exception of k_η itself—must be independent of wavenumber; i.e., like any global model the FSCK method is limited to gray surfaces and/or gray scattering properties.

Evaluation of Weight Function *a*. Note that expressing the transmissivity in terms of the correlated-*k* distribution $f(T,k)$ (second formulation in Eq. (14)) also satisfies the RTE, replacing the $[aI_b]$ in Eq. (19) by $[f(T,k)I_b]$, in which case the resulting intensity has to be integrated over *k*-space, i.e., $I=\int_0^\infty I_k dk$ [17]. The advantage of the present formulation—besides demonstrating the equivalence between *k*-distribution and the WSGG model—is the fact that the weight function $a(T,g)$ is much smoother and better behaved than the *k*-distribution, and thus requires fewer quadrature points (i.e., gray-gas evaluations) for the accurate determination of full spectrum results such as heat flux. It remains to determine the $k(T,g)$ distributions for a given gas mixture followed by transformation to $k(T_{\text{ref}},g_{\text{ref}})$, i.e., the evaluation of the $a(T,g_{\text{ref}})$. This can be done in a number of ways, the two most extreme ones being calculation from (i) total emissivity (transmissivity) data, and (ii) from line-by-line data such as the HITRAN [23,24] or HITEMP [25] databases. In this paper, we will limit our consideration to high-resolution databases.

HITRAN92 [23] has been used successfully in meteorological applications, but is known to be inaccurate for combustion scenarios since many hot lines are missing in that database. HITRAN96 [24] has remedied this problem to some extent and may now be used with confidence for up to 600K, although many hot lines are still missing. Very recently, HITEMP [25] has become available for carbon dioxide and water vapor and should be accurate for up to 1000 K. However, it has many times the number of spectral lines than HITRAN96, requiring substantially more computer time, and is limited to carbon dioxide and water vapor mixtures. In either case $k(T,g)$ is determined from Eqs. (14) or (24) for a fixed reference condition. Recall that the temperature dependence in $k(T,g)$ originates from the fractional Planck function *i*, *not* from the absorption coefficient, which is evaluated at the reference condition (which remains fixed). The transformation function $a(T,g)$ is best determined by ratioing the slopes of the (preferably slightly smoothened) *g* distribution functions for the actual and the reference temperature for the same *k*, since *a* may have discontinuities if $f(T,k)/f(T_{\text{ref}},k)$ is employed (since the *f* may have singularities, albeit at identical *k*-values). Once the correlated-*k* distribution and the weight function have been determined, the temperature and additional pressure dependence given by the function $u(T,p,\underline{x})$ in Eq. (5) must be postulated and/or determined in some optimal way.

There are several different ways to obtain $k(T,g)$ from line-by-line data as described in several papers [2,3,21,26]. We prefer the following method, which is simple, quick, adaptive and particularly well-suited for full-spectrum calculations: the spectrum $0\leqslant\eta<\infty$ is subdivided into *N* equal subintervals, and $N+1$ equally spaced spectral locations. Similarly, the *k*-range is subdivided into *J* ranges (because of the large order-of-magnitude range of the absorption coefficient, the *k*-range is subdivided equally on a $\log_{10}k$-basis). A set of temperatures T_i can be considered simultaneously. A scan is now made over the $N+1$ spectral locations, the local value of *k* is calculated, and the j^{th} *k*-bin for the i^{th} temperature T_i is incremented by the corresponding fractional Planck function if $k_j\leqslant k<k_{j+1}$, i.e., $I_{b\eta}\delta\eta$, with a resolution fine enough that $I_{b\eta}(T_i)$ is constant across $\delta\eta$. At the end of the scan all bin values are multiplied by $\pi/\sigma T_i^4$, after which they reflect the calculated values for $f(T,k_j)\delta k_j$ and the cumulative *k*-distribution for each temperature follows from

$$g(T,k_j) = \sum_{j'=1}^{j} f(T,k_{j'})\delta k_j = g(T,k_{j-1}) + f(T,k_j)\delta k_j. \tag{29}$$

Note that the number of *k*-bins as well as temperature bins can be made arbitrarily large without any appreciable increase in computation time. While that may result in empty bins, the $g(T,k)$ distribution would simply remain constant for adjacent *j*-values. After each scan the number of *N* is doubled, resulting in *N* additional knot points, and *N* additional *k*-values are calculated and placed in the $f(T,k_j)$ bins, until such time when the g_j no longer change beyond some criterion. Note also that, in the limit of $\delta k\to 0$, $\delta\eta\to 0$, it follows that $f(T,k)\to\infty$ wherever k_η is maximum or minimum, resulting in small discontinuities for $a(T,k)$ at these points. Thus, the smoothness of *f* and *a* are strongly affected by the numerical implementation.

By making a transformation from $f(k)dk$ to the weight function $a(T,g)dg$ it was hoped to obtain a smoothened function for easier quadrature (similar to the transformation from $f(k)dk$ to dg, with $k(g)$ being a much smoother function than $f(k)$). This is demonstrated for two extreme temperatures in Fig. 2(*a*), showing $f(T_{\text{cold}},k)$, $f(T_{\text{hot}},k)$, and $a(T_{\text{cold}},k)$, using the hot gas temperature as the reference state. The corresponding $k(T,g)$, together with $a(T_{\text{cold}},g)$ are shown in Fig. 2(*b*). While the weight function $a(T,g)$ is not as smooth as the $k(T,g)$ function, *a* is considerably better behaved than the $f(T,k)$: high frequency oscillations are reduced from approximately 25 percent of maximum to about 5 percent (as discussed earlier, maxima of *f* and, therefore, *a*, depend on the numerical implementation; values given are for our present calculations). Low frequency oscillations are also much less severe. As the temperature moves closer to the reference value, *a* becomes progressively smoother (hovering around an average value of $a=1$). Therefore, accurate numerical quadrature of Eq. (20) becomes relatively easy. Efficient quadrature can be further improved by smoothing the weight function through

$$\int_0^1 a(g)\phi(k(g))dg = \int_0^1 \frac{1}{\Delta g}\int_{\Delta g} a(g')\phi(k(g'))dg'dg \simeq \int_0^1 \overline{a}(g)\phi(k(g))dg, \tag{30}$$

where

$$\overline{a} = \frac{1}{\Delta g}\int_{\Delta g} a(g')dg' \tag{31}$$

since $k(g)$ is essentially constant across a small interval Δg. In this expression $\phi(k)$ is any function that depends on *g* through the function $k(T,g)$, such as I_g. The smoothened weight function $\overline{a}$ is also indicated in Fig. 2(*b*) along with typical quadrature points used in later examples. Also indicated are typical step values k_i for the WSGG trapezoidal integration.

Scaling of Absorption Coefficient. The FSCK method is exact as compared to LBL calculations that use the same scaled

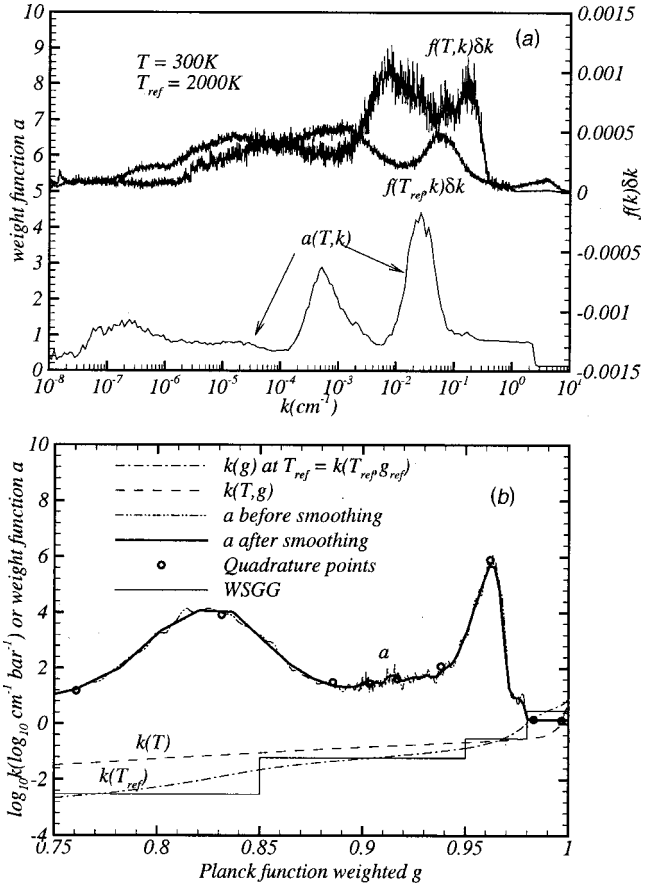

Fig. 2 (*a*) Comparison of *k*-distributions at different temperatures and the weight function *a*, (*b*) Planck function weighted cumulative *k*-distribution *g*, and the weight function *a*

absorption coefficient. Errors arise only from the fact that actual gas mixtures do not obey the scaling approximation. Therefore, optimal scaling methodology is extremely important for the accuracy of the FSCK method, although this remains somewhat of a black art. While the FSCK method is, in principle, valid for arbitrary gas mixtures, we will limit ourselves here to systems with constant total pressure, which reduces the determination of a scaled absorption coefficient distribution from a line-by-line database to two steps. First, a reference condition must be chosen. Assuming constant total pressure throughout, it appears natural to take a volume average as the reference mole fraction distribution, or

$$\underline{x}_{\mathrm{ref}}=\frac{1}{V}\int_V \underline{x}\,dV. \tag{32}$$

Choosing an optimal reference temperature is less obvious; different possibilities are listed and discussed as follows:

Maximum Temperature in System.

$$T_{\mathrm{ref}}=T_{\mathrm{hot}} \tag{33a}$$

Minimum Temperature in System.

$$T_{\mathrm{ref}}=T_{\mathrm{cold}} \tag{33b}$$

Volume Averaged Temperature.

$$T_{\mathrm{ref}}=\frac{1}{V}\int_V T\,dV \tag{33c}$$

Planck Mean Temperature.

$$(\kappa_P T^4)_{\mathrm{ref}}=\frac{1}{V}\int_V \kappa_P T^4\,dV \tag{33d}$$

Emission Weighted Temperature.

$$T_{\mathrm{ref}}=\frac{\int_V T[4\sigma\kappa_P(T,p,\underline{x})T^4]dV+\int_A T[\epsilon\sigma T^4/\pi]dA}{\int_V[4\sigma\kappa_P(T,p,\underline{x})T^4]dV+\int_A[\epsilon\sigma T^4/\pi]dA} \tag{33e}$$

Since at the reference state the absorption coefficient is set to coincide with that of the database, an intermediate temperature may be expected to do better than choosing the maximum (Eq. (33*a*)) or minimum temperatures (Eq. (33*b*)) as the reference temperature, such as a spatially averaged temperature (Eq. (33*c*)). However, straight volume averaging neglects local variations in mole fractions, as well as the fact that emission from hot regions often dominates the radiative field. Therefore, using a Planck mean temperature (based on overall emitted energy) or an emission-weighted temperature can be expected to give better results. The performance of different reference temperatures will be tested later within this paper.

Once a reference state has been established, an appropriate spatial variation function $u(T,p,\underline{x})$ must be found. If we assume constant total pressure throughout the system and neglect pressure effects on the line half widths b_j (generally a good approximation for systems with roughly constant total pressure), then spectral lines become temperature and pressure dependent through only the line intensities S_j, which, for a linear absorption coefficient, is linearly proportional to the partial pressure of the absorbing gas, times a function of temperature only.

Since radiative heat fluxes from a layer are governed by emission rates attenuated by self absorption, the scaling function for a gas mixture with only one participating gas $u(T,x)$ is found here from the implicit relation

$$\int_0^\infty I_{b\eta}(T_{\mathrm{em}})\exp[-\kappa_\eta(T,x)L_m]d\eta = \int_0^\infty I_{b\eta}(T_{\mathrm{em}})\exp[-k_\eta u(T,x)L_m]d\eta, \tag{34}$$

where $k_\eta=\kappa_\eta(T_{\mathrm{ref}},x_{\mathrm{ref}})$ and L_m is the mean beam length of the volume under consideration. Note that there are two temperatures involved in Eq. (34), an emission temperature T_{em} and the reference temperature T_{ref}. Using an emission temperature different from T_{ref} may give better results, but will involve a larger amount of precalculations and interpolations. For simplicity, one may consider the use of the reference temperature also as the emission temperature. For optically thin situations, Eq. (34) ensures that the scaling produces the correct Planck-mean absorption coefficient at all locations (weighted by T_{em}). For optically thick situations, Eq. (34) ensures that the scaling produces the correct heat flux escaping a layer with a thickness of L_m. For gas mixtures with more than one participating gas specie, we use here an assumed shape of

$$u(T,\underline{x})=\sum_{n=1}^{N} x_n u_n(T), \tag{35}$$

where $x_n u_n(T)$ is the scaling function for the n^{th} gas specie and is evaluated, independently for each specie, using Eq. (34). This simplification has the disadvantage that it neglects line overlap between species (in the function of optimal scaling parameters only, *not* in the heat transfer calculations). It has the advantage that the volumetric scaling function can be databased independently for each specie.

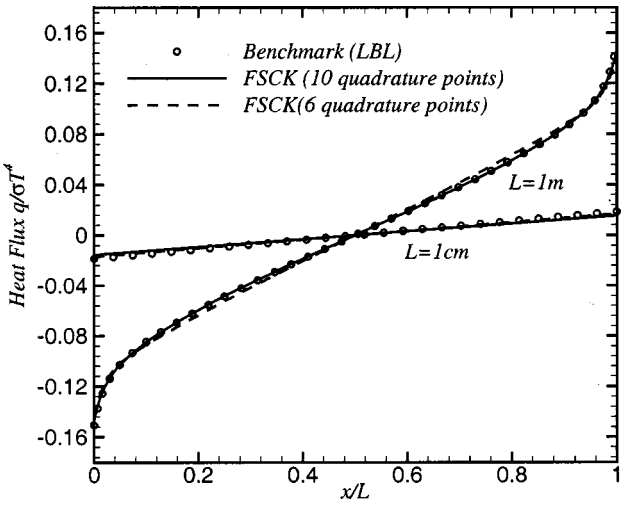

Fig. 3 Local radiative flux in an isothermal N_2–CO_2 mixture (T=1500 K, p=1 bar, x_{CO_2}=0.1, L=1 cm and L=1 m) bounded by cold, black walls

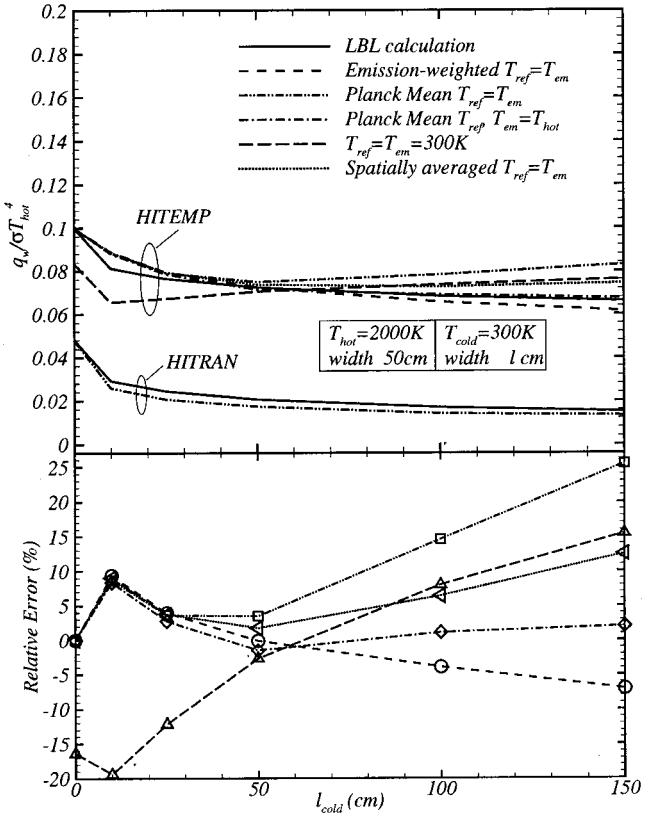

Fig. 4 Radiative flux exiting from the cold column of a two-column CO_2-nitrogen mixture at different temperatures (T_{hot}=2000 K, l_{hot}=50 cm; T_{cold}=300 K, l_{cold} variable; uniform p=1 bar, x_{CO_2}=0.1, cold and black walls) using HITEMP and HITRAN96 databases; the relative errors shown are for HITEMP results

Sample Calculations

The validity of the present model, its application to non-black walls and scattering media, and its limitations due to the scaling approximation will be shown through a number of relatively simple one-dimensional examples in which CO_2-N_2 mixtures confined between two infinite parallel walls are considered. Also, a two-dimensional practical combustion problem will be studied to test the model, with more than one participating gas coexisting in a cylindrical axisymmetric combustion chamber. The P_1 approximation is employed in the following examples, since it is a popular method with reasonable levels of effort and accuracy. Since the FSCK method is a spectral model that can be used with any RTE solution method, comparison of the LBL benchmark with FSCK demonstrates the accuracy of the FSCK method as long as the same RTE solver is employed in both cases. Any other solution method than the P_1 approximation would also be acceptable. The HITEMP as well as HITRAN96 databases are used in the following calculations to validate the new approach, and methods to determine optimally scaled absorption coefficients will be discussed.

One-Dimensional Slab. First an isothermal medium confined between two parallel, cold and black plates is considered. Since the medium is homogeneous, the *k*-distribution at only one temperature is needed, i.e., at the temperature of the medium, so that $a \equiv 1$ in this case. The medium is a nitrogen-carbon dioxide mixture at 1500 K, 1 bar total pressure, with a 10 percent mole fraction of CO_2. Using the HITEMP database for the evaluation of absorption coefficients, benchmark line-by-line results are compared in Fig. 3 with the Full-Spectrum Correlated-*k* Distribution (FSCK) method for two slab widths demonstrating that the FSCK method is indeed exact for homogeneous media. Using 10 Gaussian quadrature points, the FSCK results essentially coincide with the LBL results (for which approximately 600,000 quadrature points were needed). Using only 6 quadrature points shows slight discrepancies for optically thick cases (L=1 m). Similar to LBL calculations, more accurate results can be obtained by using more quadrature points. Within numerical accuracy, the wall heat flux predicted by the FSCK is exact for the homogeneous and isothermal case.

Taine et al. [22] have shown that the scaling approximation may produce substantial errors when radiation emitted in a hot region travels through a cold layer, since (i) *k*-distributions always sort absorption coefficients according to magnitude (assuming that this produces consistent wavenumber sorting), while (ii) in strongly non-isothermal media this ordering consistency is violated by "hot lines," which have large absorption coefficients at high temperatures, while being essentially negligible at low temperatures. We will consider two types of non-isothermal media. First, we will look at the extreme case of an isothermal hot layer adjacent to an isothermal cold layer. This extreme test will allow us to find out optimum ways to determine accurately scaled absorption coefficient distributions from the HITEMP database. Figure 4 shows the radiative heat flux arriving at the cold black wall of a N_2-CO_2 mixture with a step in temperature. Pressure and CO_2 mole fraction are constant throughout at 1 bar and 10 percent, respectively. The hot layer is at T=2000 K and has a fixed width of 50 cm, while the cold layer is at 300 K, and is of varying width. The LBL results obtained from both the HITEMP and the HITRAN96 databases are compared with various scaling approximations. Note that heat fluxes predicted from the HITEMP database are more than double (no cold layer) to five-fold (thick cold layer) of those predicted from the HITRAN96 database: while the HITRAN96 database can be used with confidence up to about 600 K [27], for temperatures beyond that level it appears to be missing many hot lines, which are estimated in the HITEMP database. Since FSCK requires quadrature over a single monotonically increasing function and needs about 10 quadrature points, while LBL calculations require about 1 million quadrature points, the FSCK method will greatly speed up the calculations. In this example, based on a well-established absorption coefficient database for both FSCK and LBL, the FSCK calculations required less than 0.05 second (10 quadrature points) on an SGIO200 (single processor R10000 at 150 MHz), while the LBL calculations required 25 minutes, or a factor of approximately 100,000:1.

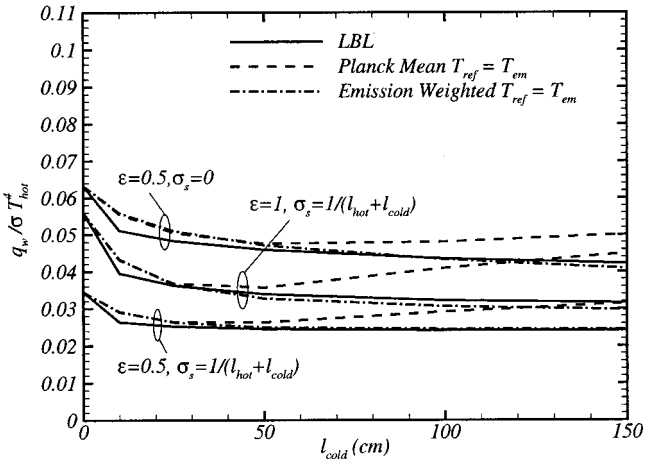

Fig. 5 Same as Fig. 4, but for medium bounded by gray walls as well as for gray scattering media

From Fig. 4 it can be seen that using two temperature scaling (T_{hot} as T_{em} in Eq. (34), plus a Planck mean reference temperature) gives the best results with a maximum error of only 8 percent. In this problem, the emission weighted temperature is very close to the hot temperature of 2000 K and, using it for both T_{em} and T_{ref}, gives a maximum error of 9 percent. Using the spatially averaged temperature and the cold temperature (300 K) as T_{ref} and T_{em} gives maximum errors of 13 percent and 19 percent, respectively. Using the Planck mean temperature for both T_{ref} and T_{em} produces a maximum error of 25 percent for this extreme temperature case because, with increasing cold layer, the Planck-mean reference temperature moves closer to the cold temperature, greatly overpredicting emission from the hot layer. Although producing large errors in this extreme example, we feel that the Planck mean temperature, together with the emission-weighted temperature, are the best choices for reference temperature. As will be shown later, Planck mean and emission-weighted temperatures are actually very close in more realistic combustion systems.

Denison and Webb [11] have already shown that the WSGG method is applicable to gray boundaries. To demonstrate that the FSCK method and, therefore, also the WSGG method is equally valid not only for media bounded by gray walls, but also for (gray) scattering media, heat fluxes through the mixture of the previous example were also calculated for the cases of gray walls (ϵ=0.5), the addition of a gray scattering medium (scattering coefficient $\sigma_s = 1/(l_{\text{hot}} + l_{\text{cold}})$), and the combination of both. The choice of σ_s here is arbitrary, and is chosen to give an optical thickness of unity, where one would expect scattering to have the largest effects. Representative calculations using line-by-line calculations together with the scaled absorption coefficient confirmed that the FSCK method produces exact results (for the scaled absorption coefficient), even in the presence of non-black walls and gray scattering. In all cases using the emission-weighted temperature as the reference value gave again the most accurate results. Inspection of Fig. 5 shows that with the presence of a nonblack wall the heat flux to the wall is reduced and the maximum relative error remains approximately the same. The influence of scattering and combined effects are also shown in Fig. 5. Qualitatively, the trends remain the same, with maximum errors at $l_{\text{cold}} = 10$ cm of 9.5 percent and 10.4 percent, respectively. Again, HITEMP results as compared to HITRAN96 results are higher by a factor of 2 (no cold layer) to about 6 (thick cold layer).

The previous examples with a step change in temperature were designed to be a worst-case scenario, i.e., to understand the limits of the scaling approximation, and as a tool to find methods to determine optimum scaling parameters for a gas mixture. One-dimensional nitrogen-carbon dioxide mixtures with smoothly

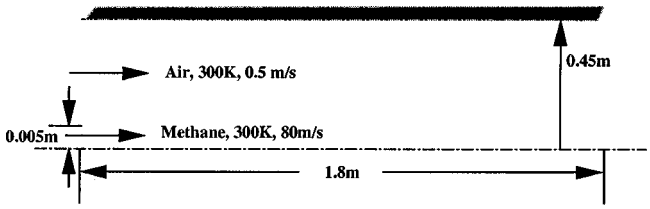

Fig. 6 Geometry of the cylindrical combustor

varying temperature and/or mole fraction profiles, such as one may expect to occur in actual combustion applications, make LBL and FSCK results virtually coincide [28].

Two-Dimensional Gas Mixtures. The model will now be tested further by applying it to a practical combustion problem. A mixture of combustion products (i.e., CO_2 and H_2O) as well as fuel (i.e., CH_4) in a cylindrical axisymmetric geometry is studied, as shown in Fig. 6. A small nozzle at the center of the combustor introduces methane at high speed and ambient air enters the combustor coaxially at a lower speed. Fuel and air mix and are allowed to react using a simple eddy dissipation reaction model. The liner wall is assumed black and insulated, and its temperature is equal to the local gas temperature. Since fuel is injected from the inlet together with cold air, temperatures near the inlet are relatively low (≅300 K). The combustion reaction produces a bell-shaped flame sheet with high downstream outlet temperatures. Temperature levels inside the chamber range from 300 K to around 1700 K, as shown in Fig. 7(*a*). The mole fraction distri-

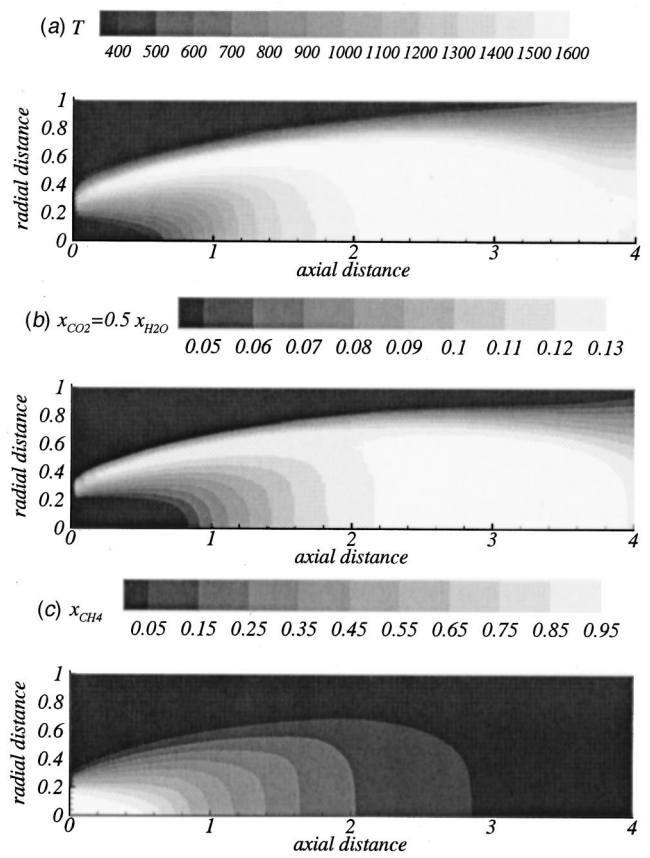

Fig. 7 Temperature and mole fraction distribution in a two-dimensional cylindrical combustion chamber, (*a*) temperature distribution; (*b*) mole fraction distribution of CO_2 and H_2O; and (*c*) mole fraction distribution of CH_4 (gas mixtures with methane and without methane are both considered).

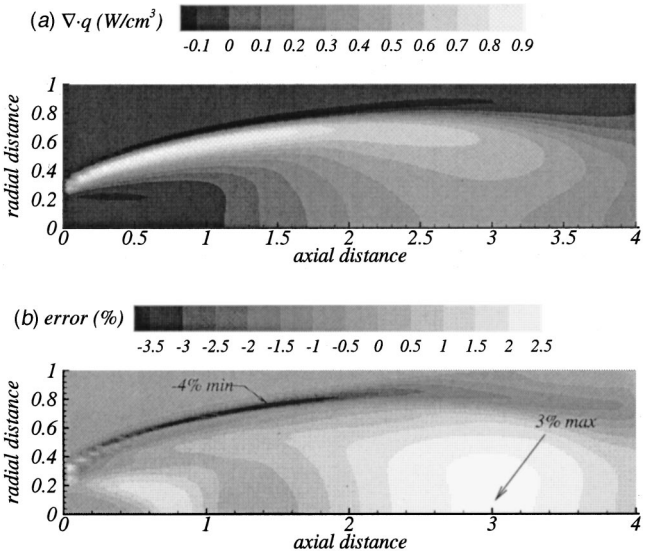

Fig. 8 Two-dimensional cylindrical combustion chamber with a gas mixture containing CO_2 and H_2O: (*a*) LBL calculations for the radiative heat source $\nabla\cdot\mathbf{q}$ (W/cm^3); (*b*) relative error of FSCK results, $(\nabla\cdot q_{\mathrm{LBL}}-\nabla\cdot q_{\mathrm{FSCK}})/\nabla\cdot q_{\mathrm{LBL,max}}$.

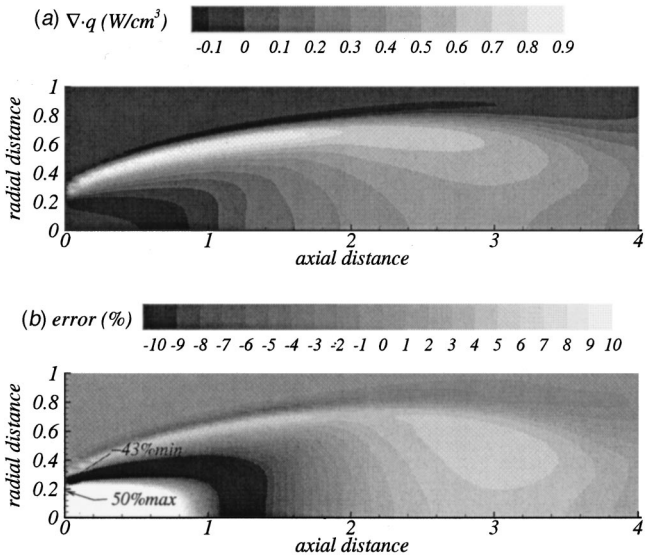

Fig. 9 Two-dimensional cylindrical combustion chamber with a gas mixture containing CO_2, H_2O and CH_4: (*a*) LBL calculations for the radiative heat source $\nabla\cdot\mathbf{q}$ (W/cm^3); (*b*) relative error of FSCK results, $(\nabla\cdot q_{\mathrm{LBL}}-\nabla\cdot q_{\mathrm{FSCK}})/\nabla\cdot q_{\mathrm{LBL,max}}$.

bution of the combustion products basically follows the pattern of the temperature change, as shown in Fig. 7(*b*), with $x_{\mathrm{H_2O}}=2x_{\mathrm{CO_2}}$ everywhere (using a simple global reaction for methane). The fuel, on the other hand, has large mole fractions near the inlet where it has not yet been consumed, and is barely present beyond where combustion has taken place, as shown in Fig. 7(*c*). LBL calculations were carried out as a benchmark. Since three emitting and absorbing gases coexist in this chamber (in this case, methane, carbon dioxide and water vapor), the FSCK approach needs now to be applied to a gas mixture of more than one participating gas. In the following calculations, the reference and emission temperatures in Eq. (34) are taken as the Planck mean temperature. Choosing the emission weighted temperature from Eq. (33*e*) instead, yields essentially the same results, since both temperatures are very close to each other.

We will first consider the case of CO_2 and H_2O being the only radiatively participating gases, with the temperature distribution shown in Fig. 7(*a*) and mole fraction distribution shown in Fig. 7(*b*). Although the mole fractions of the combustion products vary throughout the volume, the mole fraction ratios of CO_2 to H_2O is 0.5 everywhere. The radiative heat source $\nabla\cdot\mathbf{q}$ determined from LBL calculations for this case is shown in Fig. 8(*a*) and the relative error of the FSCK method with respect to the LBL benchmark, defined as

$$\mathrm{error(percent)}=\frac{\nabla\cdot\mathbf{q}_{\mathrm{LBL}}-\nabla\cdot\mathbf{q}_{\mathrm{FSCK}}}{\nabla\cdot\mathbf{q}_{\mathrm{LBL,max}}}\times 100 \qquad (36)$$

is shown in Fig. 8(*b*). It can be seen that the maximum errors are around -4 percent across the sharp gradients just outside the flame sheet, and $+3$ percent in the hot downstream section. Thus, one may conclude that the FSCK method predicts heat transfer rates very well in situations where gases have constant ratios of mole fraction. In this problem, the CPU time required for LBL calculations is about 60 h, while that for the FSCK method is 5 sec.

Next we consider the same mixture of CO_2 and H_2O, but will also include the radiative participation of CH_4. Since methane, as the fuel, has large mole fractions only near the inlet as shown in Fig. 7(*c*), the gases in the mixture no longer have the same mole fraction ratio throughout the combustion chamber. Again, LBL calculations are carried out as a benchmark and are shown in Fig. 9(*a*). The distribution of the radiative heat source differs from the previous problem only in the inlet region because of the presence of CH_4. Shown in Fig. 9(*b*), the maximum error of the FSCK approach now increases to 50 percent in the inlet region with its mole fraction discontinuity, although the error remains well below 10 percent throughout most of the combustion chamber. It can be seen that non-constant ratios of mole fraction of participating gases have a big effect on the accuracy of the method, since at one location gas ''*a*'' may be prominent, and gas ''*b*'' at another, causing severe breakdown of absorption coefficient scaling. To overcome this problem we have also developed a multi-scale FSCK method [29].

Summary and Conclusions

A Full-Spectrum Correlated-*k* Distribution (FSCK) has been developed, which—within its limitations (gray walls, gray scattering, spectral absorption coefficient obeying the scaling approximation)—allows very efficient ''exact'' evaluation of radiative fluxes for arbitrary molecular gas mixtures, using any desired RTE solver. Nongray surfaces and/or nongray scattering would require a multi-band approach (rather than full-spectrum). It has been shown that the popular Weighted-Sum-of-Gray-Gases (WSGG) method is simply a crude implementation of the FSCK method; therefore, it is implied that the WSGG method can also be applied to gray enclosures as well as gray scattering media. Limitations of the scaling approximation have also been investigated and procedures to find optimally scaled distributions have been discussed. Comparison of results using the HITRAN96 and HITEMP databases shows that, beyond 1000 K, HITEMP radiative fluxes are several times larger than those from HITRAN, thus indicating the application limits of HITRAN96.

Acknowledgments

The authors gratefully acknowledge the financial support of the National Science Foundation under the contract CTS-9615009. Temperature and mole fraction profiles for the axisymmetric combustion problem in Fig. 7 were provided by Mr. G. Li.

Nomenclature

A = weight function for WSGG method

a = weight function for FSCK method
b = line half-width, cm^{-1}
f = k-distribution function, cm
g = cumulative k-distribution
I = radiative intensity, W/m^2sr
i = fractional Planck function
k = absorption coefficient variable, cm^{-1}
k_η = spectral absorption coefficient at reference state, cm^{-1}
l = geometric length, m
L_m = mean beam length, m
p = pressure, bar
q = radiative heat flux, W/m^2
S = line intensity, cm^{-2}
s, s' = distance along path, m
T = temperature, K
u = spatial dependence function for absorption coefficient
V = Volume, m^3
X = weighted path length, m
$x, \underline{x}$ = mole fraction, mole fraction vector

Greek Symbols

α = absorptivity
ϵ = emissivity
η = wavenumber, cm^{-1}
Φ = scattering phase function
κ = absorption coefficient, cm^{-1}
Ω = solid angle, sr
σ_s = scattering coefficient, cm^{-1}
τ = transmissivity

Subscripts

0 = reference condition
b = blackbody emission
em = emission
i = gray gas in WSGG
j = line or bin
P = Planck mean
w = wall
η = spectral

References

[1] Goody, R., West, R., Chen, L., and Crisp, D., 1989, "The Correlated-*k* Method for Radiation Calculations in Nonhomogeneous Atmospheres," J. Quant. Spectrosc. Radiat. Transf., **42**, No. 6, pp. 539–550.

[2] Lacis, A. A., and Oinas, V., 1991, "A Description of the Correlated-*k* Distribution Method for Modeling Nongray Gaseous Absorption, Thermal Emission, and Multiple Scattering in Vertically Inhomogeneous Atmospheres," Journal of Geophysical Research, **96**, No. D5, pp. 9027–9063.

[3] Fu, Q., and Liou, K. N., 1992, "On the Correlated-*k* Distribution Method for Radiative Transfer in Nonhomogeneous Atmospheres," J. Atmos. Sci., **49**, No. 22, pp. 2139–2156.

[4] Rivière, Ph., Soufiani, A., and Taine, J., 1992, "Correlated-*k* and Fictitious Gas Methods for H_2O Near 2.7 μm," J. Quant. Spectrosc. Radiat. Transf., **48**, pp. 187–203.

[5] Rivière, Ph., Scutaru, D., Soufiani, A., and Taine, J., 1994, "A New CK Data Base Suitable From 300 K to 2500 K for Spectrally Correlated Radiative Transfer in CO_2-H_2O-Transparent Gas Mixtures," in *Proceedings of the 10th International Heat Transfer Conference*, ed., G. F., Hewitt, Taylor & Francis, London.

[6] Rivière, Ph., Soufiani, A., and Taine, J., 1995, "Correlated-*k* and Fictitious Gas Model for H_2O Infrared Radiation in the Voigt Regime," J. Quant. Spectrosc. Radiat. Transf., **53**, pp. 335–346.

[7] Soufiani, A., and Taine, J., 1997, "High Temperature Gas Radiative Property Parameters of Statistical Narrow-Band Model for H_2O, CO_2 and CO, and Correlated-*k* Model for H_2O and CO_2," Int. J. Heat Mass Transf., **40**, No. 4, pp. 987–991.

[8] Hottel, H. C., and Sarofim, A. F., 1967, *Radiative Transfer*, McGraw-Hill, New York.

[9] Modest, M. F., 1991, "The Weighted-Sum-of-Gray-Gases Model for Arbitrary Solution Methods in Radiative Transfer," ASME J. Heat Transfer, **113**, No. 3, pp. 650–656.

[10] Denison, M. K., and Webb, B. W., 1993, "An Absorption-Line Blackbody Distribution Function for Efficient Calculation of Total Gas Radiative Transfer," J. Quant. Spectrosc. Radiat. Transf., **50**, pp. 499–510.

[11] Denison, M. K., and Webb, B. W., 1993, "A Spectral Line Based Weighted-Sum-of-Gray-Gases Model for Arbitrary RTE Solvers," ASME J. Heat Transfer, **115**, pp. 1004–1012.

[12] Denison, M. K., and Webb, B. W., 1994, "*k*-Distributions and Weighted-Sum-of-Gray Gases: A Hybrid Model," in *Tenth International Heat Transfer Conference*, Taylor & Francis, London, pp. 19–24.

[13] Denison, M. K., and Webb, B. W., 1995, "The Spectral-Line-Based Weighted-Sum-of-Gray-Gases Model in Nonisothermal Nonhomogeneous Media," ASME J. Heat Transfer, **117**, pp. 359–365.

[14] Denison, M. K., and Webb, B. W., 1995, "Development and Application of an Absorption Line Black-Body Distribution Function for CO_2," Int. J. Heat Mass Transf., **38**, pp. 1813–1821.

[15] Denison, M. K., and Webb, B. W., 1995, "The Spectral-Line Weighted-Sum-of-Gray-Gases Model for H_2O/CO_2 Mixtures," ASME J. Heat Transfer, **117**, pp. 788–792.

[16] Rivière, Ph., Soufiani, A., Perrin, Y., Riad, H., and Gleizes, A., 1996, "Air Mixture Radiative Property Modelling in the Temperature Range 10000-40000 K," J. Quant. Spectrosc. Radiat. Transf., **56**, pp. 29–45.

[17] Pierrot, L., Rivière, Ph, Soufiani, A., and Taine, J., 1999, "A Fictitious-Gas-Based Absorption Distribution Function Global Model for Radiative Transfer in Hot Gases," J. Quant. Spectrosc. Radiat. Transf., **62**, pp. 609–624.

[18] Pierrot, L., Soufiani, A., and Taine, J., 1999, "Accuracy of Narrow-Band and Global Models for Radiative Transfer in H_2O, CO_2, and H_2O-CO_2 Mixtures at High Temperature," J. Quant. Spectrosc. Radiat. Transf., **62**, pp. 523–548.

[19] Modest, M. F., 1993, *Radiative Heat Transfer*, McGraw-Hill, New York.

[20] Goody, R. M., and Yung, Y. L., 1989, *Atmospheric Radiation—Theoretical Basis*, 2nd ed., Oxford University Press, New York.

[21] Goody, R., West, R., Chen, L., and Crisp, D., 1989, "The Correlated-*k* Method for Radiation Calculations in Nonhomogeneous Atmospheres," J. Quant. Spectrosc. Radiat. Transf., **42**, pp. 539–550.

[22] Taine, J., and Soufiani, A., 1999, "Gas IR Radiative Properties: From Spectroscopic Data to Approximate Models," in *Advances in Heat Transfer*, **33**, Academic Press, New York, pp. 295–414.

[23] Rothman, L. S., Gamache, R. R., and Tipping, R. H. et al., 1992, "The HITRAN Molecular Database: Editions of 1991 and 1992," J. Quant. Spectrosc. Radiat. Transf., **48**, No. 5/6, pp. 469–507.

[24] Rothman, L. S., Rinsland, C. P., Goldman, A., Massie, S. T., Edwards, D. P., Flaud, J. M., Perrin, A., Camy-Peyret, C., Dana, V., Mandin, J. Y., Schroeder, J., McCann, A., Gamache, R. R., Wattson, R. B., Yoshino, K., Chance, K. V., Jucks, K. W., Brown, L. R., Nemtchinov, V., and Varanasi, P., 1998, "The HITRAN Molecular Spectroscopic Database and HAWKS (HITRAN Atmospheric Workstation): 1996 Edition," J. Quant. Spectrosc. Radiat. Transf., **60**, pp. 665–710.

[25] Rothman, L. S., Camy-Peyret, C., Flaud, J.-M., Gamache, R. R., Goldman, A., Goorvitch, D., Hawkins, R. L., Schroeder, J., Selby, J. E. A., and Wattson, R. B., 2000, "HITEMP, the High-Temperature Molecular Spectroscopic Database," J. Quant. Spectrosc. Radiat. Transf., to appear.

[26] Arking, A., and Grossman, K., 1972, "The Influence of Line Shape and Band Structure on Temperatures in Planetary Atmospheres," J. Atmos. Sci., **29**, pp. 937–949.

[27] Modest, M. F., and Bharadwaj, S., 2001, "High-Resoultion, High-Temperature Transmissivity Measurements and Correlations for Carbon Dioxide-Nitrogen Mixtures," in *Proceedings of the ICHMT 3rd International Symposium on Radiative Transfer*, Antalya, Turkey.

[28] Modest, M. F., and Zhang, H., 2000, "The Full-Spectrum Correlated-*k* Distribution and Its Relationship to the Weighted-Sum-of-Gray-Gases Method," in *Proceedings of the 2000 IMECE*, **HTD-366-1**, Orlando, FL, ASME, New York, pp. 75–84.

[29] Modest, M. F., and Zhang, H., 2002, "A Multi-Level Full-Spectrum Correlated-*k* Distribution for Radiative Heat Transfer in Inhomogeneous Gas Mixtures," J. Quant. Spectrosc. Radiat. Transf., in print.